Structure of *Bombyx mori* Silk Fibroin Based on the DFT Chemical Shift Calculation

Ping Zhou,* Guiyang Li, Zhengzhong Shao, Xiaoyun Pan, and Tongyin Yu

Contribution from The Key Laboratory of Molecular Engineering of Polymers, Ministry of Education, Macromolecular Science Department, Fudan University, Shanghai 200433, P. R. China

Received: July 5, 2001; In Final Form: September 11, 2001

Despite extensive investigation of *Bombyx mori* silk fibroin structures by many experimental methods, e.g., X-ray diffraction, molecular modeling calculation, and solid static ^{13}C NMR spectroscopy, a set of fingerprint structural parameters remains unavailable both for the silk I and the silk II forms. In this study, a density functional theory (DFT) approach was used to assess available structural parameters on the basis of the comparison of calculated^{13}C chemical shifts or shielding tensors with experimental data. The results indicate that: (i) the silk I form, first proposed in this work, is a 3_1-helixlike conformation with torsion angle ranges of $\langle\varphi\rangle = -59 \pm 2°$, $\langle\psi\rangle = 119 \pm 2°$, and $\langle\omega\rangle = 178 \pm 2°$ for the alanine residue and $\langle\varphi\rangle = -78 \pm 2°$, $\langle\psi\rangle = 149 \pm 2°$, and $\langle\omega\rangle = 178 \pm 2°$ for the glycine residue in the silk fibroin; and (ii) the silk II structures independently determined by Marsh, Fossey, and Asakura are considered to be more rational than those determined by other authors. The resulting torsion angle ranges for the silk II form are $\langle\varphi\rangle = -143 \pm 6°$, $\langle\psi\rangle = 142 \pm 5°$, and $\langle\omega\rangle = 178 \pm 2°$ both for Ala and Gly residues.

1. Introduction

In addition to the exceptional mechanical properties of *Bombyx mori* silk which have been widely studied extensivily,[1−4] the structural feature of silk fibroin also attracts attention because its understanding may explain the origin of silk fibroin macroscopic behaviors. The primary structure of *B. mori* silk fibroin has been determined to be composed dominantly of a six-amino acid-residue motif, i.e., −Gly−Ala−Gly−Ala−Gly−Ser−.[5] Although there exist two crystalline domains, silk I and silk II, reported on the basis of X-ray diffraction,[6−10] molecular modeling calculations,[11,12] ^{13}C solid-state NMR spectroscopy,[13−19] etc., a definitive answer on silk fibroin structure remains unclear. It is generally accepted[6,19,20] that the basic feature of silk II proposed by Marsh et al.[6] in 1955 is an orderly packing of antiparallel β-pleated sheets with unit cell dimensions of $a_0 = 9.40$ Å, $b_0 = 6.97$ Å, $c_0 = 9.20$ Å, and $\beta = 90°$ and hydrogen bond length of 2.78 Å in the β-pleated sheets. However, Takahashi et al.[8,21] revised this earlier model on the basis of a more detailed X-ray diffraction analysis with 35 quantitative intensities. They clarified that the crystalline domain of the silk II bears rather random stacking of antipolar−antiparallel sheets, in which the methyl groups (β-carbon) of alanine residues alternately point to both sides of the protein chain, which is different from the crystal structure where all the methyl groups point to the same side of the protein chain.[6] Moreover, Lazo et al.[12] discovered a new form of β-helical conformation based on the molecular modeling calculation for the silk fibroin. They indicated that all side groups of amino acids are arrayed on the exterior of the β-helix single-chain and ascribed it to a silk II form. For the conformation of the silk I form, its structural parameters remain unclear because this less stable conformation is highly susceptible to transformation into the silk II conformation, leading to difficulty in performing X-ray diffraction experiments. Lotz and Keith[9] proposed a crankshaft model with a unit cell of 4.72 × 14.4 × 9.6 Å in which Ala and Gly residues are close to the β-sheet and α-helix conformations, respectively. Furthermore, Konishi and Kurokawa[10] proposed a loose 4-fold helical conformation with a unit cell of 4.59 × 7.20 × 9.08 Å whose residue translation is 2.27 Å. Although He et al.[22] recently redetermined the X-ray diffraction experiment for a silk I sample, the determined unit cell parameters of 22.66 × 5.70 × 20.82 Å are evidently different from those of the two previous structures. Also, they are also different from that (8.94 × 6.46 × 11.26 Å) calculated by Fossey[11] via the molecular modeling approach. Lazo[12] also proposed a four-residue β-turn structure based on the molecular energy calculation and applied it to a silk I form. We find that all of the above proposed models have quite different structural parameters (see Table 3) although they are all regarded as either the silk I or the silk II form. On the other hand, Valluzzi[23,24] reported the third crystal structure of *B. mori* silk fibroin, termed as silk III, which was observed on an ultrathin film formed at an air−water interface. This new structure indicates a trigonal symmetry based on the X-ray diffraction results. It thus prompts us to consider a question of which structural models may be more rational for *B. mori* silk fibroin.

A bridge between calculation and experimentation, such as NMR chemical shift, is becoming an especially useful tool for determining molecular structures.[25] Local variations in angles, bond lengths, and environment can contribute to chemical shifts.[26] Experimentally, many correlations between shift and local conformation have been established, such as between shifts of C^α and C^β atoms and backbone torsion angles in protein.[27−29] The connection between structure and shielding tensors (or chemical shifts) implies that chemical shifts should be calculable if structure were known and, vice versa, structure should be predictable if shifts were known.[30] In fact, quantum chemical calculation of chemical shielding tensors has made great progress during the past few years.[31−34] In particular, the use of the density functional theory (DFT) has greatly reduced the computational cost and has made the investigation of larger

* To whom corresponding should be addressed. E-mail: pingzhou@fudan.edu.cn. Tel: +86-21-65642866. Fax: +86-21-65640293.

10.1021/jp0125395 CCC: $20.00
Published on Web 11/20/2001

TABLE 1: Various Silk Fibroin and Polypeptide Samples with Their Preparation Conditions

sample no.[a]	sample type	sample preparation conditions	refs
I	cocoon	Extracted directly from silk cocoon.	13
II	degummed silk	Cocoon was degummed with boiling aqueous Na_2CO_3 solution.	our work
III	crystalline fraction	Precipitated from aqueous solution treated with chymotrypsin.	13
IV	crystalline fraction	Like sample **III** but measured with a higher resolution of ^{13}C NMR.	16
V	β-sheet crystalline fraction of *P. c. ricini*	Precipitates of *P. c. ricini* fibroin digested by chymotrypsin.	16
VI	β-sheet $(Ala)_n$	Oligo(L-alanines) with $n < 8$.	45
VII	β-sheet $(Gly)_n$	With Mw = 6000.	13
VIII	crystalline fraction	Precipitates resulting from the dialysis of 9 mol/l LiBr solution of sample **III** crystalline fraction against distilled water containing ethylic acid (pH < 5).	16
IX	regenerated fibroin (solid)	Solid from casting the regenerated fibroin solution (which was obtained by dissolving the degummed *B. mori* silk into 9 mol/l LiBr solution and then dialyzing the solution against distilled water).	our work
X	regenerated fibroin (liquid)	Collected supernatant from the regenerated solution.	43
XI	Gland in larva (liquid)	Concentrated fibroin gel stored in the abdominal gland of *B. mori* mature larva.	43
XII	α-helical *P. c.ricini* fibroin	Casting the liquid fibroin directly taken from the posterior silk gland of the mature larva onto PMMA plate.	16
XIII	random $(Ala)_n$	Copolymer of l- and d- polyalanines.	45
XIV	α-helix $(Ala)_n$	Poly(L-alanines) with $n > 16$.	45
XV	3_1-helix $(Gly)_n$	Average DP (degree of polymerization) = 50.	44

[a] Samples **I**−**V** were ascribed as silk II form by the literature authors (these samples are water-insoluble), while samples **VIII**−**XII** were ascribed as the silk I form, which is water-soluble.

systems possible.[35,36] The computed shielding values for the first- and second-row elements were very close to the experimental values[31,37] when gauge-included atomic orbitals (GIAO)[38] or individual gauge localized orbitals (IGLO)[39] methods were used. Some structures of amino acids,[34,40,41] small polypeptides,[31,34] and proteins[30,36,42] have been predicted or refined via chemical shift calculation by ab initio as well as DFT methods.

Accordingly, in this paper, we tried to theoretically identify and deduce the *B. mori* silk fibroin structure in light of the conformation-dependent ^{13}C chemical shift. We calculated ^{13}C shielding tensors and chemical shifts of silk fibroin with various available structural parameters via GIAO method at DFT level and compared the calculated results with experimental values. Consequently, we attempted to rationalize the fibroin structures determined previously by experimental and theoretical approaches. The idea combined with NMR spectroscopy and quantum chemical calculation of chemical shift would provide a powerful tool in the investigation of molecular structures for which no single-crystal X-ray structure is available.[25]

2. Methods

Experimental Data. There are many ^{13}C NMR spectroscopic studies on silk fibroin both in solution and in the solid state. Table 1 summarizes various silk fibroin and silk-like polypeptide samples with their preparation conditions, and Table 2 summarizes the experimental chemical shifts of samples cited from previous literatures[13−16,43,44,45] and those reported by us. ^{13}C CP-MAS NMR spectra were recorded under the conditions as reported in ref 14, e.g., ^{13}C nuclear magnetic resonance at 75.5 or 100.7 MHz with contact time of 800u, pulse repeat time of 1s, and accumulation of scans over 1500. Samples **I**−**VII** are considered to correspond to the fibroin silk II form (which is water-insoluble) or polypeptide β-sheet conformation, whereas samples **VIII**−**XV** to the fibroin silk I form (which is water-soluble) or polypeptide helix conformations.

Moreover, a series of structural dihedral angles of silk fibroin based on previous studies[6,10−12,14,18,19,21,24] are also collected in Table 3. The molecular structures presented in this report were built up using SYBYL[46] with (i) the default values of bond lengths and bond angles of amino acids available in this software and (ii) the dihedral angles of silk fibroin in Table 3. The constructed geometries of fibroin conformations remain fixed during the chemical shift calculation.

TABLE 2: Summary of Isotropic ^{13}C Chemical Shift of Experiments for Silk Fibroins and Silk-like Polypeptides

sample no.	conformation	Ala			Gly		ref
		C^α	C^β	C=O	C^α	C=O	
I	silk II	49.7	20.2	171.7	43.9	169.4	13
II	silk II	48.6	20.2	172.2	43.1	169.6	our work
III	silk II	48.7	18.9	170.7	43.0	169.4	13
IV	silk II	49.4	20.2	172.3	43.1	169.5	16
V	β-sheet	48.6	20.0	171.8	42.8	168.8	16
VI	β-sheet	48.2	19.9	171.8			13, 45
VII	β-sheet				43.2	168.4	13
VIII	silk I	51.4	16.5	177.0	43.8	170.7	15
IX	silk I	49.7	15.8	172.5	43.0	172.5	14
		51.6	17.0	172.6	43.8	172.6	our work
X	silk I	50.0	16.6	175.5	42.7	171.5	43
XI	silk I	50.0	16.7	175.5	42.6	171.5	43
XII	α-helix	52.5	15.7	176.2	43.0	172.3	16
XIII	random	51.1	15.7	176.1			45
XIV	α-helix	52.4	14.9	176.4			13, 45
XV	3_1-helix				42.0	172.1	44

TABLE 3: Summary of Various Available Conformation Torsion Angles of *B. Mori* Silk Fibroin

structure no.	Ala			Gly			conformation	refs
	φ	ψ	ω	φ	ψ	ω		
1	−139	140	180	−139	140	180	silk II	6
2	−150	149	179	−152	148	177	silk II	11
3	−140	142	180	−139	135	180	silk II	19
4	−180	180	180	−180	180	180	β-sheet	
5	−141	152	165	−140	153	165	silk II	21
6	160	−107	180	163	−82	180	silk III	24
7	−105	112	180	80	50	180	Crankshaft (left-handed)	28
8	−125	88	180	−50	−76	180	Crankshaft (right-handed)	28
9	−26	135	180	−26	135	180	loose-helix	10, 14
10	−58	−47	180	−58	−47	180	3.6_{13}-helix	46
11	−73	85	180	137	−84	180	β-helix	12
12	−59	119	180	64	29	180	β-turn	12
13	−80	150	180	−150	80	178	silk I	11
14	−80	150	180	−80	150	180	3_1-helix	14,63
15	−59	119	180	−78	149	180	silk I	our work

Quantum Chemical Calculations. ^{13}C chemical shielding tensors were calculated using GIAO at the hybrid DFT level

with the B3LYP (Becke's three-parameter hybrid method of Lee, Yang and Parr) exchange-correlation functional as implemented in *Gaussian* 98.[47] This functional comprises both local and nonlocal exchange contributions and contains terms accounting for local and nonlocal correlation corrections. The standard *Gaussian* basis set 6-311G(d,p), which includes one set of d-type polarization function on the heavy atoms and one set of p-type polarization function on the hydrogen atoms, was adopted for all the ^{13}C atom calculations. For the calculations of all other atoms, the basis set 6−31(d,p) was used. B3LYP/6-311G(d, p) have been successfully applied in predicting energy,[48] chemical shift,[49,50] infrared frequencies,[51,52] etc., for many systems, such as peptide,[30] nucleic acids[49] as well as metal complexes.[50] All the calculated ^{13}C chemical shifts in the present work are referenced to the shielding constant of TMS ^{13}C atom.[53] All the calculations in this work were performed on Pentium III computers and a Down-1000A high-performance computing system equipped with 16 processors.

3. Results and Discussion

A correlation between chemical shift and silk fibroin conformation can be clearly seen in Figure 1. In Table 2, from samples **I**−**V**, which were assigned to fibroin silk II form (being dominant of β-sheetlike conformation), the experimental chemical shifts in Ala residues of C^{α} fall in the range of 48.2−49.7 ppm, of C^{β} within 18.9−20.2 ppm, and of carbonyl carbon within 170.7−172.3 ppm. The chemical shifts of these samples are comparable with that of model polypeptide $(Ala)_n$ (sample **VI**), whereas for samples **VIII**−**XII**, which were assigned to fibroin silk I form (being dominant of random coil and helix conformations), the chemical shifts of C^{α} in Ala residues lie slightly downfield at 50.0−52.5 ppm when compared with that formed in silk II or β-sheet conformation. The chemical shifts of C^{β} in Ala residues lie in a higher magnetic field (within 15.7−17.0 ppm) than that in silk II. Similarly, when carbonyl carbons are compared, the chemical shift values of silk I (within a large variation range of 172.5−177.0 ppm depending upon the different sample preparation conditions) are higher than those of silk II. These chemical shift-dependences on the conformations are also observed in the model polypeptides, such as samples **XIII** and **XIV**, which are dominated by random coil and helix conformation. However, the chemical shifts of C^{α} in Gly residues do not appear significantly different between silk I and silk II forms with their chemical shifts within the region of 42.0−43.9 ppm for all the fibroin samples as well as model polypeptides $(Gly)_n$ (samples **VII** and **XV**). The chemical shifts of carbonyl carbons in Gly residues also show the trends similar to that observed in the Ala residues; i.e., carbonyl carbon chemical shifts lie to a higher magnetic field (from 168.4 to 169.6 ppm) for the silk II form compared to that of the silk I form (from 170.7 to 172.6 ppm). In fact, this correlation exists not only in above systems but also in $(Leu)_n$, $(Val)_n$, $(Ile)_n$[54], and other polypeptides[14,27] and proteins.[28,29]

By analyzing above experimental NMR spectra and considering that experimental errors are within ±0.5 ppm, it is possible to distinguish the chemical shifts of silk I from silk II. The chemical shifts of C^{α} and C^{β} in Ala residue is suggested to be within 48.0−50.0 ppm and 18.5−20.5 ppm, respectively, for silk II and within 50.0−53.0 ppm and 14.5−17.5 ppm, respectively, for silk I. The chemical shift of C(C═O) in Ala residue is within 170.0−172.5 ppm for silk II form. Yet the chemical shift of C (C═O) in Ala residue for the silk I form varies significantly depending upon the sample preparation conditions. Note that there exists higher chemical shift value

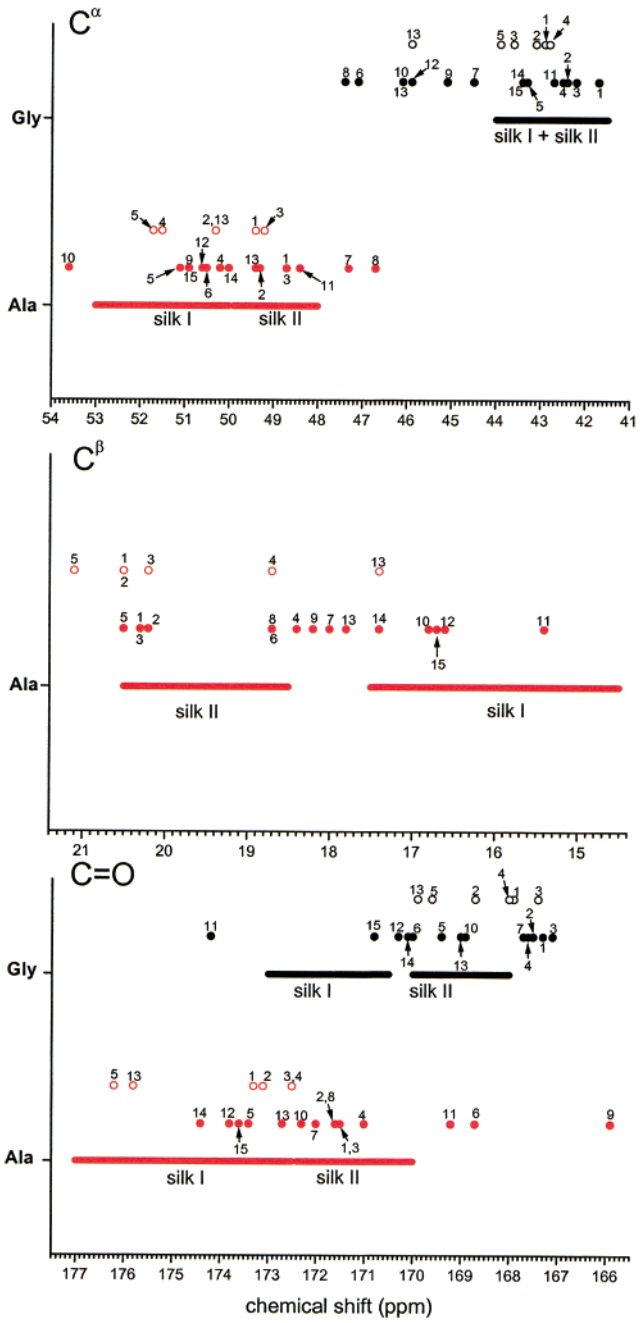

Figure 1. ^{13}C chemical shift distributions. Bold lines indicate the chemical shift ranges of silk I and silk II forms extracted from experimental ^{13}C NMR spectra. Solid circles (●) were extracted from the calculated ^{13}C chemical shifts for all the available silk fibroin structures, and open circles (○) were the values for the hydrogen-bond-involved structures.

when the sample is in aqueous solution (∼175.5 ppm) when compared with that in the anhydrous solid state (∼172.6 ppm). This similar behavior was observed and investigated previously in detail when anhydrous *B. mori* fibroin solid was gradually hydrated under a highly moisture atmosphere for several days.[16] Therefore, the chemical shift of C (C═O) in Ala residue should be within 172.5−177.0 ppm for silk I form. Both silk I and silk II have similar C^{α} chemical shifts, falling within 41.5−44.0 ppm in Gly residues. Moreover, silk I has a higher C═O chemical shift within 170.5−173.0 ppm in Gly residues, whereas for silk II, they are within 168.0−170.0 ppm. These classifications are drawn as bold lines in Figure 1. Therefore, it is possible to calculate their chemical shifts and compare the calculated

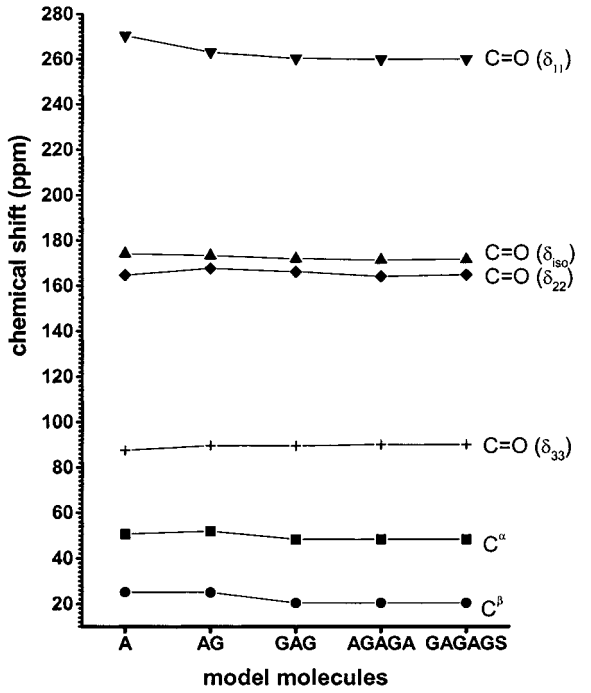

Figure 2. Influence of polypeptide chain lengths on ^{13}C chemical shifts and shielding tensors of functional groups in the alanine residue.

results with experimental values through which the various proposed structural models of *B. mori* silk fibroin may be rationalized. Since chemical shift-dependences on the structures are similar between small biomolecules and biomacromolecules,[40,55,56] here we attempt to expand a rational small polypeptide as a structural model for the large silk fibroin system based on the DFT chemical shift calculation. To achieve this goal, the following procedures are involved to obtain a convincing conclusion.

Effects of Backbone Lengths on the Chemical Shifts. Because chemical shift is sensitive to the local environmental changes rather than the changes in the entire molecule,[14] it is necessary to choose a molecular size suitable to represent a general silk fibroin system without requiring prohibitively expensive computational resources. The effect of the molecular chain lengths on the ^{13}C isotropic chemical shifts and their shielding components was thus explored. We calculated the chemical shifts using DFT method for the model molecule $NH_2-L-Ala-NH_2$ (A) and silk-like polypeptide models (i.e., residue capped with an acetyl group at the C-terminus and an amide group at the N-terminus) $NH_2-L-Ala-Gly-H$ (AG), $NH_2-Gly-L-Ala-Gly-H$ (GAG), $NH_2-L-Aly-Gly-L-Ala-Gly-L-Ala-H$ (AGAGA), and $NH_2-Gly-L-Ala-Gly-L-Ala-Gly-Ser-H$ (GAGAGS). The torsion angles φ, ψ, and ω were fixed at $-139°$, $135°$, and $180°$, respectively, for Gly residues and $-140°$, $142°$, and $180°$, respectively, for Ala residues. This set of torsion angles, proposed by Asakura,[19] is one of the conformation parameters of silk II. As seen from Figure 2 (detail data in Table S1 of Supporting Information), provided only that the central Ala residue is considered, the chemical shifts of C^α, C^β, and C (C═O) in the sequences GAG, AGAGA, and GAGAGS are basically consistent except in the shorter amino acid A or dipeptide AG. Therefore, the model molecule AGAGA or GAGAGS is appropriate to represent a single chain of silk fibroin and could be computed efficiently.

Effect of Hydrogen Bond Lengths on Chemical Shifts. There exist many hydrogen bonds to bear the protein folding and unfolding. They may contribute to the shielding depending

SCHEME 1: Array of a Model Polypeptide AGAGA and $CH_3CONHCH_3$[a]

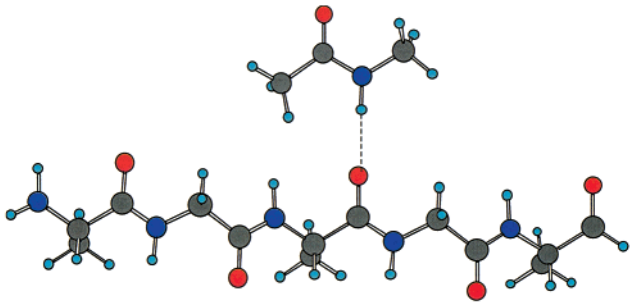

[a] H-bond is shown by dashed line.

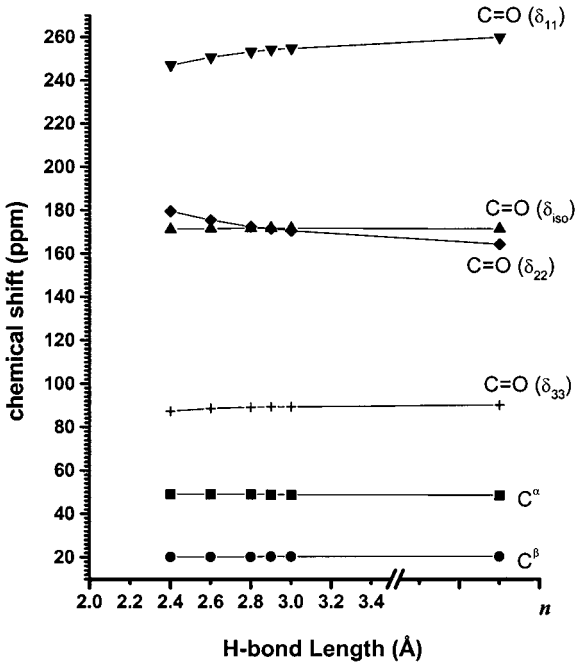

Figure 3. Influence of hydrogen bond lengths on ^{13}C chemical shifts and shielding tensors of functional groups in the alanine residue. *n* indicates AGAGA chain alone, without intermolecule hydrogen bond formed.

on the extent of the interaction. The central Ala residue in the silk-like polypeptide model AGAGA (with the same torsion angles as that in the preceding text) was chosen for the investigation of hydrogen bond effect on the chemical shifts. The hydrogen bond was considered to form between carbonyl oxygen atom of Ala in polypeptide and nitrogen atom in methylamine (Scheme 1). The orientation of the hydrogen bond coincided with the C═O bond axis, and the hydrogen bond angle of O**...**H−N was allowed to tend to 180°. The results in Figure 3 (detail data in Table S2 of Supporting Information) demonstrate that the ^{13}C isotropic chemical shifts of C^α, C^β, and even C (C═O) are essentially unaffected (within 0.2−0.6 ppm) despite a variation of the hydrogen bond length from 2.4 to 3.0 Å. However, the chemical shielding anisotropy changed considerably, especially for the components δ_{11} and δ_{22}. It is seen from Figure 3 that δ_{11} is larger than 260 ppm, while δ_{22} is smaller than 165 ppm when the hydrogen bond is not accounted for (see the points when hydrogen bond length > 3.5 Å in Figure 3). Once the hydrogen bond is taken into account (hydrogen bond length < 3.0 Å), the δ_{11} and δ_{22} change inversely; i.e., δ_{11} becomes smaller than 255 ppm (the largest difference reaches to 12.8 ppm between the two cases, i.e., with and without hydrogen bond involved), and δ_{22} becomes larger than

170 ppm (with the largest difference reaching 15.8 ppm between the two cases, i.e., with and without hydrogen bond involved) for the Ala residue. δ_{33} is relatively insensitive to the presence of hydrogen bond and exhibits a shift difference of 2.8 ppm after hydrogen bond is involved. This result suggests that the orientation of δ_{33} is most possibly perpendicular to the N−C═O plane. δ_{22}, which is moving toward the lower magnetic field when hydrogen bond is involved, is close to the C═O orientation, i.e., hydrogen bond orientation, and as a consequence, δ_{11} is thus orthogonal to both δ_{22} and δ_{33}.[57] We also considered the effect with more hydrogen bonds acting on the central Ala residue using a model such as methylamine (NH_2-CH_3) and acetaldehyde (CH_3CHO) molecules arrayed at the two sides of the GAG chain, forming two hydrogen bonds with carbonyl and amide in Ala residue (see Scheme S1 in Supporting Information). The hydrogen bond lengths were allowed to vary from 2.6 to 3.2 Å, and the results showed that the calculated chemical shift trend (data are shown in Table S3 in Supporting Information) agrees with that observed in the model system of Scheme 1.

Chemical Shift-Dependence on Structure. Experiments and theoretical calculations have shown that almost 100% of shielding change is dominated by changes in torsion angles rather than bond length and peptide sequences.[41] Therefore, in the present work, we adopted the sequence GAGAGS as a model to represent the silk fibroin molecule in the calculation of its ^{13}C chemical shifts and shielding tensors using DFT method. The different sets of structural parameters reported in the literatures for silk I as well as silk II are collected in Table 3.

The conformations of structures **1** to **5** in Table 3 were considered to be the silk II or β-sheet form. Among them, structure **1** was determined by Marsh[6] and refined again by Fraser.[7] Also, the integrity of this structure was reasserted by static ^{13}C and ^{15}N solid-state NMR experiments performed by Asakura[19] (structure **2**). Fossey et al.[11] calculated the silk II fibroin structure (structure **3**) and determined an alternative set of structural parameters (see Table 3). For these three structural models, it can be seen from Figure 1 that the calculated chemical shifts (●) for C^α, C^β, and C (C═O) in the Ala residue fall within the experimentally determined ^{13}C chemical shift region for silk II, while that in Gly residues approach the silk II region (see Figure 1). Structure **4** is a typical β-sheet conformation with uniform 180° torsion angles of φ, ψ, and ω. Its calculated chemical shifts deviate from the experimental values for the silk II form, e.g., with a little higher chemical shift value of C^α (50.2 ppm) and lower value of C^β (18.4 ppm) in the Ala residue. The ^{13}C chemical shifts corresponding to structure **5** revised by Takahashi[8,21] deviate significantly from the silk II experimental values. In particular, the Ala residue in structure **5** gave the higher chemical shift values for C^α (51.1 ppm) and C (C═O) (173.4 ppm) which lie in the silk I region, whereas the chemical shift value of C^β (20.5 ppm) in the Ala residue and that of C^α (43.3 ppm) and C (C═O) (169.4 ppm) in the Gly residue lie in the silk II region (see Figure 1). Structure **6** was determined by Valluzzi.[24] It is found that this so-called silk III form has chemical shifts significantly different from both silk I and silk II. It is, therefore, concluded that the structures **1**−**3** could plausibly be the most likely structures (with $\langle\varphi\rangle = -143 \pm 6°$, $\langle\psi\rangle = 142 \pm 5°$, and $\langle\omega\rangle = 178 \pm 2°$ for both Ala and Gly residues[58]) corresponding to silk II type *B. mori* silk fibroin, while structures **4**−**6** should be excluded from the silk II form.

Structures **7** and **8** were thought to be silk I form by Lotz and Keith.[9] They individually correspond to the left-handed (L-) and right-handed (D-) crankshaft models. However, the calculated chemical shifts showed that these two models cannot represent the silk I form. For the alanine residues, they have lower chemical shift values for C^α (47.3 and 46.7 ppm, respectively) and the carbonyl carbon (172.0 and 171.6 ppm, respectively) but higher values for C^β (18.0 and 18.7 ppm, respectively). For the glycine residues, they have higher chemical shifts for C^α (44.5 and 47.4 ppm, respectively) but lower values for the carbonyl carbon (167.7 and 164.0 ppm, respectively). Structure **9** was estimated by Saitô et al.[14] within the framework of a loose-helix conformation first proposed by Konishi and Kurokawa.[10] Again, this structure is not in agreement with experiment based on the results of chemical shift calculations. In particular, the much lower Gly C (C═O) chemical shift value (160.8 ppm) extends beyond the *X*-axis scale in Figure 1. Structure **10** is a typical 3.6_{13}-helix conformation. The results of calculated chemical shifts do not fully agree with experimental values for the silk I form. Moreover, Lazo et al.[12] proposed a β-helix conformation (structure **11**) and thought it resembled the silk II form, but the calculated chemical shifts for this structure differ significantly from experimental values for silk II form. Evidently, the chemical shift of the C (C═O) atom is even smaller (169.2 ppm) in the Ala residue than that (174.2 ppm) in the Gly residue, and the values of C^α and C^β are close to neither that of the silk I nor the silk II form.

Structure **12** proposed by Lazo[12] was considered to be a β-turn conformation and also thought to be a silk I form. The calculated chemical shifts for C^α (50.6 ppm), C^β (16.6 ppm), and C (C═O, 173.8 ppm) in the Ala residue lie in the experimental region of the silk I form (see Figure 1), but for that of C^α (45.9 ppm) in the Gly residue, it is much higher than the experimental value. Structure **13** was determined by Fossey[11], and the calculated chemical shifts of 49.4, 17.8, 172.7 ppm for C^α, C^β, and C (C═O), respectively, in the Ala residue and 169.0 ppm for C (C═O) in the Gly residue do not agree with that of the experimental silk I form quite well, particularly the higher C^α chemical shift value (46.1 ppm) in the Gly residue. But this type of silk I structure was demonstrated to be authentic by Asakura et al.[18] on the basis of the conformation-dependent chemical shift contour plots proposed by Spera and Bax.[28] Structure **14** has a 3_1-helix conformation that actually exists in many systems, such as spider silk,[59] silk-like polypeptide analogues,[60−64] and other biomacromolecules[65,66] and polymers.[67] The calculated chemical shifts for this helix (which has torsion angles of −80°, 150°, 180°[14,63] corresponding to φ, ψ, and ω, respectively, in both Ala and Gly residues) are 50.0 (C^α), 17.4 (C^β), and 174.7 (C═O) ppm for the Ala residue and 43.4 (C^α) and 170.1 (C═O) ppm for the Gly residue. These values are consistent with that of the silk I form, except for the C (C═O) of Gly, whose value is slightly lower (170.1 ppm). Accordingly, we proposed structure **15** to be a new model with the torsion angles referenced from structures **12**−**14**, whose chemical shifts are close to that of the experimental silk I region (see Figure 1). By varying torsion angles within the arrangement of −49° to −88° for φ, 110° to 155° for ψ, and 175° to 180° for ω as well as comparing the resulting chemical shifts with experimental values, a set of structural parameters for structure **15** was finally determined to be $\langle\varphi\rangle = -59 \pm 2°$, $\langle\psi\rangle = 119 \pm 2°$, and $\langle\omega\rangle = 178 \pm 2°$ for the Ala residue and $\langle\varphi\rangle = -78 \pm 2°$, $\langle\psi\rangle = 149 \pm 2°$, and $\langle\omega\rangle = 178 \pm 2°$ for the Gly residue.[58] The calculated chemical shifts corresponding to this set of parameters are 50.9 ppm (C^α), 16.7 ppm (C^β), and 173.6 ppm (C of C═O), respectively, for the Ala residue and 43.4 ppm (C^α) and 170.8 ppm (C of C═O), respectively, for the Gly residue. These results are in good agreement with the silk I form

SCHEME 2: Three-Chain Layer of a Polypeptide GAGAGS Model[a]

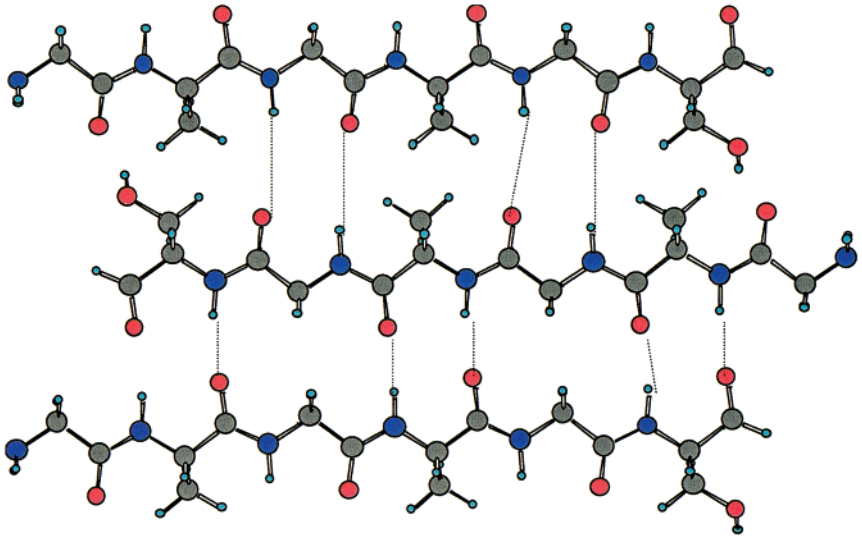

[a] H-bonds are shown by dashed lines.

TABLE 4: Summary of Calculated ^{13}C Chemical Shifts and Shielding Tensors (in ppm) for Various Available Structures of *B. mori* Silk Fibroin[a]

		Ala						Gly					
				C=O					C=O				
structure no.	conformation	C^α	C^β	δ_{iso}	δ_{11}	δ_{22}	δ_{33}	C^α	δ_{iso}	δ_{11}	δ_{22}	δ_{33}	structural data resources
1	silk II	48.7	20.3	171.5	259.8	164.4	90.3	41.7	167.3	257.2	154.3	90.4	6
		(49.8)	(20.8)	(172.5)	(260.8)	(167.1)	(89.6)	(43.8)	(168.0)	(258.0)	(156.6)	(89.5)	
	H-bond	49.4	20.5	173.3	253.8	175.3	90.9	42.9	167.9	249.5	162.7	91.6	
2	silk II	49.3	20.2	171.6	259.0	165.3	90.5	42.4	167.5	256.4	155.4	90.7	11
	H-bond	50.3	20.5	173.1	248.9	178.8	91.5	43.1	168.7	249.9	164.1	92.0	
3	silk II	48.7	20.3	171.5	259.9	164.3	90.3	42.2	167.1	257.0	153.9	90.3	19
	H-bond	49.2	20.2	172.5	249.2	177.6	90.8	43.6	167.4	246.8	164.3	91.0	
b	silk II	-	-	174.7	242	186	96	–	174.3	245	179	99	19
4	β-sheet	50.2	18.4	171.0	256.2	166.3	90.4	42.5	167.6	253.8	158.3	90.9	46
	H-bond	51.5	18.7	172.5	247.6	177.5	92.3	42.8	168.0	251.7	160.5	91.8	
5	silk II	51.1	20.5	173.4	261.9	167.1	91.3	43.3	169.4	258.4	158.0	91.8	21
	H-bond	51.7	21.1	176.2	256.3	179.8	92.6	43.9	169.6	249.4	166.8	92.8	
6	silk III	50.5	18.7	168.7	259.7	159.1	87.2	47.1	170.0	257.1	161.2	91.6	24
7	Crankshaft	47.3	18.0	172.0	263.3	162.2	90.8	44.5	167.7	258.4	156.5	88.1	18
8	Crankshaft	46.7	18.7	171.6	262.1	160.0	91.7	47.4	164.0	260.3	144.1	87.6	18
9	loose-helix	50.9	18.2	165.9	262.8	144.1	90.9	45.1	160.8	259.9	132.2	90.5	10, 14
10	3.6_{13}-helix	53.6	16.8	172.3	261.9	162.4	92.7	46.1	168.9	254.8	160.7	91.1	46
11	β-helix	48.4	15.4	169.2	261.2	148.8	97.8	42.7	174.2	245.7	187.4	89.6	12
12	β-turn	50.6	16.6	173.8	264.0	167.3	90.3	45.9	170.3	253.0	164.8	93.0	12
13	silk I	49.4	17.8	172.7	261.3	164.1	92.5	46.1	169.0	260.7	157.6	88.6	11
	H-bond	50.3	17.4	175.8	255.2	179.7	92.4	45.9	169.9	260.1	162.5	86.9	
14	3_1-helix	50.0	17.4	174.4	262.9	169.6	91.7	43.4	170.1	259.3	158.8	92.1	14, 63
15	silk I	50.9	16.7	173.6	262.3	167.3	91.1	43.4	170.8	259.3	160.3	92.9	this work
		(51.5)	(16.7)	(174.3)	(263.0)	(169.7)	(90.2)	(44.1)	(171.3)	(259.4)	(162.4)	(92.0)	

[a] The values in parentheses were calculated with basis set 6-311G(d, p) for all atoms in a model molecule. [b] Experimental results

experimental results (Figure 1). Note that the silk I or silk II torsion angle region determined by DFT chemical shift calculation for all the available structural parameters is constrained to a much narrower range than that of the α-helix or β-sheet conformations ($\langle\varphi\rangle = -62° \pm 8°$, and $\langle\psi\rangle = -42° \pm 10°$ for α-helix, while $\langle\varphi\rangle = -114 \pm 32°$ and $\langle\psi\rangle = 142° \pm 20°$ for β-sheet) determined empirically by the conformation-dependent chemical shift contour method proposed by Spera and Bax.[28] As we can see, silk I has a structure more like a 3_1-helix, while silk II has a structure falling in a certain β-sheet torsion angle region.

In addition to the single-chain model of GAGAGS, a multichain model was also adopted for the calculation. The hydrogen bonding interaction was considered to be arraying in an antiparallel arrangement for the three single-chain GAGAGS polypeptides as shown in Scheme 2. Because only structures **1**−**5** and **13** can form well-defined hydrogen bonds with 2.8−3.0 Å bond lengths between carbonyl oxygens and amide nitrogens and without close contact atoms between two adjacent chains, the hydrogen bond effect on the chemical shifts was calculated for these model structures. The calculated results[68] are summarized in Table 4. Similar to that reported in the model system (Scheme 1), the effects of hydrogen bond on the ^{13}C isotropic chemical shifts of C^α and C^β for these structures are very small (less than 1.0 ppm), but that of the carbonyl C (C=O) is relatively large, with a variation of 0.2−3.1 ppm. Moreover, the anisotropic parts of the shielding tensors are sensitive to the hydrogen bonding interaction as well (see Table 4). Indeed, the difference between the calculated and experimental regions diminishes when hydrogen bond effect is taken

into consideration in the calculation. This is especially evident for the chemical shift of C (C═O) atom in the Gly residue of structures **1**−**3** (see Figure 1).

Asakura et al.[19] experimentally extracted the ^{13}C (C═O) shielding tensors from the static^{13}C solid-state NMR spectrum by line shape simulation method. The sample used was a well-ordered silk fiber that was thought to be in the silk II form. Their results are summarized in *b* in Table 4. Although the simulated shielding tensors for the carbonyl carbon are different from our calculated results for structures **1**−**3**, several common points are present between experiments and calculations: (i) the isotropic chemical shift of C (C═O) in the Ala residue is larger than that in the Gly residue; (ii) provided that the hydrogen bond effects are considered, the calculated values of δ_{11} both in Ala and Gly residues in structures **1**−**3** are approaching that of the experimental value (242 ppm), and so are the δ_{33}; (iii) δ_{22} in the Ala residues are larger than that in the Gly residues. These three common points substantially support our calculated results. The different δ_{iso} value between theory and experiment mainly arises from the difference in values of δ_{22}. In general, the value of δ_{iso} obtained from CP-MAS experiment is more reliable than that obtained via line shape simulation for the static solid-state NMR spectrum. Therefore, if δ_{iso} obtained from CP-MAS experiments were acceptable, the shielding tensors calculated by DFT would closely approach the real shielding values.

Since the hybrid DFT exchange-correlation functional B3LYP has been demonstrated to handle the hydrogen bond system reasonable,[55,69] we tested the effect of larger basis functions on the chemical shifts under the same exchange-correlation functional in order to arrive at a more convincing conclusion,. A 6-311G(d, p) basis set was adopted for all atoms in single-chain models, i.e., structures **1** and **15**. The results show that the use of larger basis functions leads to a systematic increase in the isotropic chemical shift by 0−2.0 ppm, and the resulting chemical shift variations are kept within the experimental region of silk I or II form (see data in parentheses of Table 4). In addition, a diffusion functional-involved basis set 6-311++G-(d, p)[69] was also used to evaluate the ^{13}C isotropic chemical shift. The calculated results show (Table S4 of Supporting Information) a systematic increase for all atoms, e.g., by 1.0−1.5 ppm for C$^{\alpha}$ and C$^{\beta}$ and by 1.0−3.0 ppm for C (C═O) when compared with the results obtained using the 6-311G(d, p) basis set. Nevertheless, these differences do not change the conclusions drawn above, but the computation time is increased by 3-fold compared with the use of the 6-311G(d, p) basis set.

4. Conclusion

The silk fibroin ^{13}C chemical shifts were calculated by GIAO-DFT at B3LYP level using 6-311G(d, p) basis set. Several structures proposed by previous studies have been identified to be more rational for the silk II type *B. mori* fibroin on the basis of a comparison of ^{13}C NMR data with DFT calculation results. These structures are those proposed by Marsh (structure **1**, $\varphi = -139°$, $\psi = 140°$, and $\omega = 180°$ both for Ala and Gly residues), Asakura (structure **2**, $\varphi = -140°$, $\psi = 142°$, and $\omega = 180°$ for the Ala residue and $\varphi = -139°$, $\psi = 135°$, and $\omega = 180°$ for the Gly residue) and Fossey (structure **3**, $\varphi = -150°$, $\psi = 149°$, and $\omega = 179°$ for Ala residue and $\varphi = -152°$, $\psi = 148°$, and $\omega = 177°$ for the Gly residue). The resulting torsion angle ranges for the silk II form are $\langle\varphi\rangle = -143 \pm 6°$, $\langle\psi\rangle = 142 \pm 5°$ and $\langle\omega\rangle = 178 \pm 2°$ for both Ala and Gly residues. None of the silk I structures determined earlier has chemical shifts or shielding tensors that agree well with that characterized by ^{13}C NMR experiments. A set of new structural parameters, structure **15** (with torsion angle ranges of $\langle\varphi\rangle = -59 \pm 2°$, $\langle\psi\rangle = 119 \pm 2°$, and $\omega = 178 \pm 2°$ for the Ala residue and $\langle\varphi\rangle = -78 \pm 2°$, $\langle\psi\rangle = 149 \pm 2°$, and $\langle\omega\rangle = 178 \pm 2°$ for the Gly residue), for the silk I form has been proposed on the basis of a comparison of the structural parameters derived from structures **12**−**14**. The calculated chemical shifts of structure **15** agreed well with experimental chemical shift. More reliable structural parameters for silk I and II are difficult to obtain with the use of the present functional and basis sets although we had tried to vary torsion angles, backbone lengths, and hydrogen bonds as many as possible, and we have also considered a packing with more polypeptide chains along the three dimensions. Inherent issues such as the calculation under a vacuum environment may contribute to the disagreement between experiment data and calculated results. In addition, the earlier structural models whose chemical shifts do not agree with the experimental range may be present in silk fibroin form but not as dominant components.

Acknowledgment. This work was supported by NSFC (No. 29974004, P. R. China), NSF (No. 99ZA14001, Shanghai), the Laboratory of MRAMP (No. 991504, China), and the Foundation for University Key Teacher by the Ministry of Education. The authors wish to acknowledge Wuhan Institute of Physics and Mathematics of the Chinese Academy of Science for supplying the SYBYL software for the polypeptide building and National High Performance Computing Center (Shanghai) for funds to purchase the computation software and Dawning 1000A workstation (IBM RS/6000 compatible).

Supporting Information Available: Sample preparations and ^{13}C NMR spectra recorded in our lab; the relevant calculation data in detail as well as the comparison of basis set effect on the calculated ^{13}C chemical shifts are included. These materials are available free of charge via the Internet at http://pubs.acs.org.

References and Notes

(1) Magoshi, J.; Magoshi, Y.; Nakamura, S.; *Polym. Commun.* **1985**, *26*, 309−311.
(2) Kaplan, D. L.; Lombardi, S. J.; Muller, W. S.; Fossey, S. A. In *Biomaterials, Novel materials from Biological Sources*; Byrom, D., Ed.; Stockton Press: New York, 1991.
(3) Pérez-Rigueiro, J.; Viney, C.; Llorca, J.; Elices, M. *J. Appl. Polym. Sci.* **2000**, *75*, 1270−1277.
(4) Pérez-Rigueiro, J.; Viney, C.; Llorca, J.; Elices, M. *Polymer* **2000**, *41*, 8433−8439.
(5) Mita, K.; Ichimura, S.; Zama, M. *J. Mol. Biol.* **1988**, *203*, 917−925.
(6) Marsh, R. E.; Corey, R. B.; Pauling, L. *Biochim. Biophys. Acta* **1955**, *16*, 1−34.
(7) Fraser, R. D. B.; MacRae, T. P. *Conformations of Fibrous Proteins and Related Synthetic Polypeptides*; Academic Press: New York, l973.
(8) Takahashi, Y.; Gehoh, M.; Yuzuriha, K. *J. Polym. Sci., B: Polym. Phys.* **1991**, *29*, 889−891.
(9) Lotz, B.; Keith, H. D. *J. Mol. Biol.* **1971**, *61*, 201−215.
(10) Konishi, T.; Kurokawa, M. *Sen'i Gakkaishi* **1968**, *24*, 550−554.
(11) Fossey, S. A.; Nemethy, G.; Gibson, K. D.: Scheraga. H. A. *Biopolymers* **1991**, *3l*, 1529−1541.
(12) Lazo, N. D.; Downing, D. T. *Macromolecules* **1999**, *32*, 4700−4705.
(13) Saitô, H.; Iwanaga, Y.; Tabeta, R.; Narita, M.; Asakura, T. *Chem. Lett.* **1983**, 427−430.
(14) Saitô, H.; Tabeta, R.; Asakura, T.; Iwanaga, Y.; Shoji, A.; Ozaki, T.; Ando, I. *Macromolecules* **l984**, *17*, 1405−1412.
(15) Asakura, T.; Kuzuhara, A.; Tabeta, R.; Saitô, H. *Macromolecules* **1985**, *18*, 1841−1845.
(16) Ishida, M.; Asakura, T.; Yokoi, M.; Saitô, H. *Macromolecules* **1990**, *23*, 88−94.
(17) Saitô, H.; Ishida, M.; Yokoi, M.; Asakura, T. *Macromolecules* **1990**, *23*, 83−88.

(18) Asakura, T.; Demura, M.; Date, T.; Miyashita, N. *Biopolymers*, **1997**, *41*, 193−203.
(19) Demura, M.; Minami, M.; Asakura, T.; Cross, T. A. *J. Am. Chem. Soc.* **1998**, *120*, 1300−1308.
(20) Fraser R. D. B.; Macrae, T. P.; Stewart, F. H. C.; Suzuki, E. *J. Mol. Biol.* **1965**, *11*, 706−712.
(21) Takahashi, Y.; Gehoh, M. *Int. J. Biol. Macromol.* **1999**, *24*, 127−138.
(22) He, S. J.; Valluzzi, R.; Gido, S. P. *Int. J. Biol. Macromol.* **1999**, *24*, 187−195.
(23) Valluzzi, R.; Gido, S. P. *Biopolymers* **1997**, *42*, 705−717.
(24) Valluzzi, R.; Gido, S. P.; Zhang, W. P. *Macromolecules* **1996**, *29*, 8606−8614.
(25) Ochsenfeld, C.; Brown, S. P.; Schnell, I.; Gauss, J.; Spiess, H. W. *J. Am. Chem. Soc.* **2001**, *123*, 2597−2606.
(26) Sitkoff, D.; Case, D. A. *J. Am. Chem. Soc.* **1997**, *119*, 12262−12273.
(27) Liu A.; Riek, R.; Zahn, R.; Hornemann, S.; Glockshuber, R.; Wuthrich, K. *Biopolymers* **1999**, *51*, 145−152.
(28) Spera, S.; Bax, Ad. *J. Am. Chem. Soc*. **1991**, *113*, 5490−5492.
(29) Wishart, D. S.; Sykes, B. D.; Richards, F. M. *J. Mol. Biol*. **1991**, *222*, 311−333.
(30) Pearson, J. G.; Le, H.; Sanders, L. K.; Godbout, N.; Havlin, R. H.; Oldfield, E. *J. Am. Chem. Soc*. **1997**, *119*, 11941−11950.
(31) Le, H.; Oldfield, E. *J. Phys. Chem.* **1996**, *100*, 6423−6428.
(32) Malkin, V. G.; Malkina, O. L.; Casida, M. E.; Salahub, D. R. *J. Am. Chem. Soc*. **1994**, *116*, 5898−5908.
(33) de Dios, A. C.; Pearson, J. G.; Oldfield, E. *J. Am. Chem. Soc*. **1993**, *115*, 9768−9773.
(34) de Dios, A. C.; Oldfield, E. *J. Am. Chem. Soc*. **1994**, *116*, 5307−5314.
(35) Zhang, R. Q.; Wong, N. B.; Lee, S. T.; Zhu, R. S.; Han, K. L. *Chem. Phys. Lett*. **2000**, *319*, 213-219.
(36) de Dios, A. C.; Pearson, J. G.; Oldfield, E. *Science* **1993**, *260*, 1491−1496.
(37) Hricovini, M.; Malkina, O. L.; Bizik, F.; Nagy, L. T.; Malkin, V. G. *J. Phys. Chem. A* **1997**, *101*, 9756−9762.
(38) Weiner, S. J.; Kollman, P. A.; Nguyen, D. T.; Case, D. A. *J. Comput. Chem.* **1986**, *7*, 230−252.
(39) Schindler, M.; Kutzelnigg, W. *J. Am. Chem. Soc.* **1983**, *105*, 1360−1370.
(40) de Dios, A. C.; Laws, D. D.; Oldfield, E. *J. Am. Chem. Soc*. **1994**, *116*, 7784−7786.
(41) Malkin, V. G.; Malkina, O. L.; Salahub, D. R. *J. Am. Chem. Soc*. **1995**, *117*, 3294−3295.
(42) Le, H.; Pearson, J. G.; de Dios, A. C.; Oldfield, E. *J. Am. Chem. Soc.* **1995**, *117*, 3800−3807.
(43) Asakura, T.; Watanabe, Y.; Uchida, A.; Minagawa, H. *Macromolecules* **1984**, *17*, 1075−1081.
(44) Kricheldorf, H. R.; Muller, D. *Macromolecules* **1983**, *16*, 615−623.
(45) Saitô, H.; Tabeta, R.; Shoji, A.; Ozaki, T.; Ando, I. *Macromolecules* **1983**, *16*, 1050−1057.
(46) SYBYL Molecular Modeling Software, Version 6.1, Tripos Inc., Missouri, USA. **1994**.
(47) Frisch, M. J.; Trucks, G. W.; Schlegel, H. B.; Scuseria, G. E.; Robb, M. A.; Cheeseman, J. R.; Zakrzewski, V. G.; Montgomery, J. A., Jr.; Stratmann, R. E.; Burant, J. C.; Dapprich, S.; Millam, J. M.; Daniels, A. D.; Kudin, K. N.; Strain, M. C.; Farkas, O.; Tomasi, J.; Barone, V.; Cossi, M.; Cammi, R.; Mennucci, B.; Pomelli, C.; Adamo, C.; Clifford, S.; Ochterski, J.; Petersson, G. A.; Ayala, P. Y.; Cui, Q.; Morokuma, K.; Malick, D. K.; Rabuck, A. D.; Raghavachari, K.; Foresman, J. B.; Cioslowski, J.; Ortiz, J. V.; Stefanov, B. B.; Liu, G.; Liashenko, A.; Piskorz, P.; Komaromi, I.; Gomperts, R.; Martin, R. L.; Fox, D. J.; Keith, T.; Al-Laham, M. A.; Peng, C. Y.; Nanayakkara, A.; Gonzalez, C.; Challacombe, M.; Gill, P. M. W.; Johnson, B. G.; Chen, W.; Wong, M. W.; Andres, J. L.; Head-Gordon, M.; Replogle, E. S.; Pople, J. A. *Gaussian 98*, revision A.1; Gaussian, Inc.: Pittsburgh, PA, 1998.
(48) Zhang, R. Y.; Lei, W. F. *J. Chem. Phys*. **2000**, *113*, 8574−8579.
(49) Xu, X. P.; Au−Yeung, S. C. F. *J. Phys. Chem. B* **2000**, *104*, 5641−5650.
(50) Xu, X. P.; Au−Yeung, S. C. F. *J. Am. Chem. Soc.* **2000**, *122*, 6468−6475.
(51) McKean, D. C. *J. Phys. Chem. A* **2000**, *104*, 8995−9008.
(52) Vázquez, J.; López J. J.; Márquez, F.; Pongor, G.; Boggs, J. E. *J. Phys. Chem. A* **2000**, *104*, 2599−2612.
(53) From *Table of TMS Absolute Shielding Values*. The absolute ^{13}C chemical shift of $\sigma_r = 182.5$ ppm was calculated by B3LYP exchange-correlation functional with a 6-311+G (2d, p) basis set, and that of other atoms were calculated by B3LYP with 6-31G(d) basis set (http://www.Gaussian.com/errata.htm).
(54) Taki, T.; Yamshita, S.; Satoh, M.; Shibata, A.; Yamashita, T.; Tabeta, R.; Saitô, H. *Chem. Lett.* **1981**, 1803−1806.
(55) Gresh, N.; Guo, H.; Salahub, D. R.; Roques, B. P.; Kafafi, S. A. *J. Am. Chem. Soc.* **1999**, *121*, 7885−7894.
(56) Patel, M. A.; Deretey, E.; Csizmadia, I. G. *J. Mol. Struct.* **1999**, *492*, 1−18.
(57) Gu, Z. T.; Zambrano, R.; McDermott, A. *J. Am. Chem. Soc.* **1994**, *116*, 6368−6372.
(58) The value indicates the average angle and standard average deviation from the torsion angles of structures **I**−**III** for silk II form; both values are extracted from the torsion angles discussed in this paper for the silk I form.
(59) Kümmerlen, J.; van Beek, J. D.; Vollrath, F.; Meier, B. H. *Macromolecules* **1996**, *29*, 2920−2928.
(60) Saitô, H.; Tabeta, R.; Shoji, A.; Ozaki, T.; Ando, I.; Miyata, T. *Biopolymers* **1984**, *23*, 2279−2297.
(61) Crick, F. H. C.; Rich, A. *Nature* **1955**, *176*, 780−781.
(62) Ramachandran, G. N.; Sasisekharan, V.; Ramakrishnan, C. *Biochim. Biophys. Acta* **1966**, *112*, 168−170.
(63) Lotz, B.; Keith, H. D. *J. Mol. Biol*. **1971**, *61*, 195−200.
(64) Muñoz-Guerra, S.; Fita, I.; Aymamí, J.; Puiggalí, J. *Macromolecules* **1988**, *21*, 3464−3468.
(65) de Sanctis, S. C.; D'Archivio, A. A.; Galantini, L.; Gavuzzo, E.; Giglio, E. *J. Chem. Soc., Perkin Trans. 2* **2000**, 403−407.
(66) Marti, D. N.; Schaller, J.; Llinas, M. *Biochemistry* **1999**, *38*, 15741−15755.
(67) Brizzolara, D.; Cantow, H. J. *Macromolecules* **1996**, *29*, 191−197.
(68) Because of computational resource limitation, the calculation for the three-chain layer was separated into two steps. First, the calculation was performed by considering the upper two chains alone and then by considering the lower two chains of this three-chain layer so that the hydrogen bond effect on both central residues, Gly and Ala, in the middle of a chain can be involved.
(69) Perczel, A.; Csaszar, A. G. *J. Comput. Chem.* **2000**, *21*, 882−900.